Measurement of the branching fraction for the decay $K_S \to \pi e \nu$

The KLOE Collaboration

A. Aloisio [b], F. Ambrosino [b], A. Andryakov [d,c], A. Antonelli [d], M. Antonelli [d], C. Bacci [e], G. Bencivenni [d], S. Bertolucci [d], C. Bini [g], C. Bloise [d], V. Bocci [g], F. Bossi [d], P. Branchini [e], S. A. Bulychjov [c], G. Cabibbo [g], R. Caloi [g], P. Campana [d], G. Capon [d], G. Carboni [a], M. Casarsa [f], V. Casavola [h], G. Cataldi [h], F. Ceradini [e], F. Cervelli [i], F. Cevenini [b], G. Chiefari [b], P. Ciambrone [d], S. Conetti [o], E. De Lucia [g], G. De Robertis [j], R. De Sangro [d], P. De Simone [d], G. De Zorzi [g], S. Dell'Agnello [d], A. Denig [d], A. Di Domenico [g], C. Di Donato [b], S. Di Falco [i], A. Doria [b], M. Dreucci [d], O. Erriquez [j], A. Farilla [e], G. Felici [d], A. Ferrari [e], M. L. Ferrer [d], G. Finocchiaro [d], C. Forti [d], A. Franceschi [d], P. Franzini [g], C. Gatti [i,1], P. Gauzzi [g], S. Giovannella [d], E. Gorini [h], F. Grancagnolo [h], E. Graziani [e], S. W. Han [d,k], M. Incagli [i], L. Ingrosso [d], W. Kluge [m], C. Kuo [m], V. Kulikov [c], F. Lacava [g], G. Lanfranchi [d], J. Lee-Franzini [d,ℓ], D. Leone [g], F. Lu [d,k] M. Martemianov [m], M. Matsyuk [d,c], W. Mei [d], A. Menicucci [a], L. Merola [b], R. Messi [a], S. Miscetti [d], M. Moulson [d], S. Müller [m], F. Murtas [d], M. Napolitano [b], A. Nedosekin [d,c], F. Nguyen [e], M. Palutan [e], L. Paoluzi [a], E. Pasqualucci [g], L. Passalacqua [d], A. Passeri [e], V. Patera [d,n], E. Petrolo [g], D. Picca [g], G. Pirozzi [b], L. Pontecorvo [g], M. Primavera [h], F. Ruggieri [j], N. Russakovic [i], P. Santangelo [d], E. Santovetti [a], G. Saracino [b], R. D. Schamberger [ℓ], B. Sciascia [g], A. Sciubba [d,n], F. Scuri [f], I. Sfiligoi [d], T. Spadaro [g,2], E. Spiriti [e], G. L. Tong [d,k], L. Tortora [e], E. Valente [g], P. Valente [d], B. Valeriani [m], G. Venanzoni [i], S. Veneziano [g], A. Ventura [h], Y. Xu [d,k], Y. Yu [d,k], P. F. Zema [i]

[a] *Dipartimento di Fisica dell'Università "Tor Vergata" e Sezione INFN, Roma, Italy.*

[b] *Dipartimento di Scienze Fisiche dell'Università "Federico II" e Sezione INFN, Napoli, Italy*

[c] *Permanent address: Institute for Theoretical and Experimental Physics, Moscow, Russia.*

[d] *Laboratori Nazionali di Frascati dell'INFN, Frascati, Italy.*

[e] *Dipartimento di Fisica dell'Università "Roma Tre" e Sezione INFN, Roma, Italy.*

[f] *Dipartimento di Fisica dell'Università e Sezione INFN, Trieste, Italy.*

[g] *Dipartimento di Fisica dell'Università "La Sapienza" e Sezione INFN, Roma, Italy.*

[h] *Dipartimento di Fisica dell'Università e Sezione INFN, Lecce, Italy.*

[i] *Dipartimento di Fisica dell'Università e Sezione INFN, Pisa, Italy.*

[j] *Dipartimento di Fisica dell'Università e Sezione INFN, Bari, Italy.*

[k] *Permanent address: Institute of High Energy Physics, CRS, Beijing, China.*

[ℓ] *Physics Department, State University of New York at Stony Brook, USA.*

[m] *Institut für Experimentelle Kernphysik, Universität Karlsruhe, Germany.*

[n] *Dipartimento di Energetica dell'Università "La Sapienza", Roma, Italy.*

[o] *Physics Department, University of Virginia, USA.*

Abstract

We present a measurement of the branching ratio BR($K \to \pi^{\pm} e^{\mp} \bar{\nu}(\nu)$) performed using the KLOE detector. K_S-mesons are produced in the reaction $e^+e^- \to \phi \to K_S K_L$ at the DAΦNE collider. In a sample of $\sim 5 \times 10^6$ K_S-tagged events we find 624 ± 30 semileptonic K_S decays. Normalizing to the $K_S \to \pi^+\pi^-$ count in the same data sample, we obtain BR($K_S \to \pi e \nu$) $= (6.91 \pm 0.37) \times 10^{-4}$, in agreement with the Standard Model expectation.

In the Standard Model, there are only $\Delta S = \Delta Q$ transitions at tree level. $\Delta S = -\Delta Q$ transitions exist at higher order, but are suppressed by a factor of $\sim 10^{-6}$–10^{-7} [1,2]. Under this assumption, together with TCP-invariance [3,4], it follows that $\Gamma(K_S \to \pi e \nu) = \Gamma(K_L \to \pi e \nu)$ to very high accuracy. Using the values of BR($K_L \to \pi e \nu$) and τ_S/τ_L from ref [5], one obtains BR($K_S \to \pi e \nu$) $= (6.70 \pm 0.07) \times 10^{-4}$. Precise measurements of the K_S semileptonic decay rate are important for checking the above assumptions. Until recently, no experimental information was available about the semileptonic decay of the K_S-meson. This is in large part due to the smallness of the branching ratio and to the difficulty of isolating $\pi^{\pm} e^{\mp} \bar{\nu}(\nu)$ decays from $\pi^+\pi^-$ decays. Both decays are observed as two charged tracks, but the latter are ~ 1000 times more abundant. Good particle identification is necessary for isolating a pure sample of $\pi^{\pm} e^{\mp} \bar{\nu}(\nu)$ events. The CMD-2 collaboration at VEPP-2M operating at the ϕ

peak has observed 75 ± 13 semileptonic K_S decays [6], with limited separation of signal and background. They find $\mathrm{BR}(K_S \to \pi e\nu) = (7.2 \pm 1.4) \times 10^{-4}$. With KLOE [7,8], we have considerably improved on this result.

Our measurement is performed with kaons from $\phi \to K_S K_L$ decays. KLOE operates at DAΦNE [9], an e^+e^- collider also known as the Frascati ϕ–factory. ϕ-mesons are produced in small angle (25 mrad) collisions of equal energy electrons and positrons, giving the ϕ a small transverse momentum component in the horizontal plane, $p_\phi \sim 13\,\mathrm{MeV}/c$. The main advantage of studying kaons at a ϕ–factory is that ϕ-mesons decay $\sim 34\%$ of the time into neutral kaons. K_L's and K_S's are produced almost back-to-back in the laboratory, with mean decay paths $\lambda_\mathrm{L} \sim 340\,\mathrm{cm}$ and $\lambda_\mathrm{S} \sim 0.6\,\mathrm{cm}$, respectively. Detection of a long-lived kaon therefore tags the production of a K_S-meson and gives its direction and momentum. The contamination from $K_L K_L \gamma$ and $K_S K_S \gamma$ final states is negligible for our measurement [10,11]. Since the branching ratio for $K_S \to \pi^+\pi^-$ is known with an accuracy of $\sim 0.4\%$ [5], the $K_S \to \pi e\nu$ branching ratio is evaluated by normalizing the number of signal events to the number of $K_S \to \pi^+\pi^-$ events in the same data set. This allows cancellation of the uncertainties coming from the integrated luminosity, the ϕ production cross section, and the tagging efficiency. Both charge states $\pi^+ e^- \bar{\nu}$ and $\pi^- e^+ \nu$ are included in the measured branching ratio. The measurement is based on an integrated luminosity of $17\,\mathrm{pb}^{-1}$ at the ϕ peak collected during the year 2000, corresponding to $\sim 5 \times 10^7$ produced ϕ-mesons.

The KLOE detector (Fig. 1) consists of a large cylindrical drift chamber surrounded by a lead-scintillating fiber sampling calorimeter. A superconducting coil outside the calorimeter provides a 0.52 T field. The drift chamber [12], 4 m in diameter and 3.3 m long, has 12 582 all-stereo sense wires and 37 746 aluminium field wires. The chamber shell is made of carbon fiber-epoxy composite and the gas used is a 90% helium, 10% isobutane mixture. These features maximize transparency to photons and reduce $K_L \to K_S$ regeneration. The position resolutions are $\sigma_{xy} \sim 150\,\mu\mathrm{m}$ and $\sigma_z \sim 2\,\mathrm{mm}$. The momentum resolution is $\sigma(p_\perp)/p_\perp \leq 0.4\%$. Vertices are reconstructed with a spatial resolution of $\sim 3\,\mathrm{mm}$. The calorimeter [13], divided into a barrel and two endcaps, covers 98% of the solid angle. The energy resolution is $\sigma_E/E = 5.7\%/\sqrt{E(\mathrm{GeV})}$ and the timing resolution is $\sigma_t = 54\,\mathrm{ps}/\sqrt{E(\mathrm{GeV})} \oplus 50\,\mathrm{ps}$. The trigger [14] uses calorimeter and chamber information. For the present analysis, the trigger relies entirely on calorimeter information. Two local energy deposits above threshold (50 MeV on the barrel, 150 MeV on the endcaps) are required. The trigger time has a large spread with respect to the bunch crossing time. It is however synchronized with the machine RF divided by 4, $T_\mathrm{sync} = 10.8\,\mathrm{ns}$, with an accuracy of 50 ps. The time T_0 of the bunch crossing producing an event is determined after event reconstruction.

About half of the K_L-mesons reach the calorimeter, where most interact. A K_L

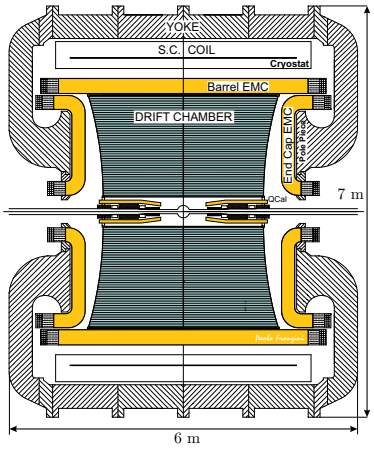

Fig. 1. Vertical cross section of the KLOE detector.

interaction is called a K_L-*crash* in the following. A K_L-crash is identified as a local energy deposit with energy above 100 MeV and a time of flight indicating low velocity: $\beta \sim 0.218$. The coordinates of the energy deposit determine the K_L's direction to $\sim$20 mrad and its momentum $\mathbf{p}_L$, which is weakly dependent on the K_L direction because of the motion of the ϕ-meson. A K_L-crash thus tags the production of a K_S of momentum $\mathbf{p}_S = \mathbf{p}_\phi - \mathbf{p}_L$. K_S-mesons are tagged with an overall efficiency of $\sim$30%. Both $K_S \to \pi e \nu$ and $K_S \to \pi^+\pi^-$ decays are selected from this tagged sample. Event selection consists of fiducial cuts, particle identification by time of flight, and kinematic closure.

Identification of $K_S \to \pi^+\pi^-$ decays requires two tracks of opposite curvature. Tracks must extrapolate to the interaction point (IP) within KLOE resolutions. The reconstructed momenta and polar angles must lie in the intervals $120\,\mathrm{MeV}/c < p < 300\,\mathrm{MeV}/c$ and $30^\circ < \theta < 150^\circ$. A cut in $(p_\perp, p_\parallel)$ selects non-spiralling tracks. 1 636 604 $K_S \to \pi^+\pi^-$ events have been found. Contamination due to K_S decays other than $K_S \to \pi^+\pi^-$ is well below the per-mil level and is ignored.

Identification of $K_S \to \pi e \nu$ events also begins with two tracks of opposite curvature. Tracks must extrapolate *and form a vertex* at the IP. The invariant mass $M_{\pi\pi}$ of the pair calculated assuming both tracks are pions must be smaller than 490 MeV. This rejects $\sim$95% of the $\pi^+\pi^-$ decays.

Electrons and pions are discriminated by time of flight (TOF). Tracks are therefore required to be associated with calorimeter energy clusters. For each track, we compute the difference $\delta_t(m) = t_{\mathrm{cl}} - L/c\beta(m)$ using the cluster time t_{cl} and the track length L. The velocity β is computed from the track momentum for each mass hypothesis, $m = m_e$ and $m = m_\pi$. In order to avoid uncertainties due to the determination of T_0, we make cuts on the two-track difference

$$d\delta_{t,\mathrm{ab}} = \delta_t(m_a)_1 - \delta_t(m_b)_2,$$

where the mass hypothesis $m_{a(b)}$ is used for the track 1(2). This difference is zero for the correct mass assignments. An additional fraction of $K_S \to \pi^+\pi^-$ events is rejected by requiring $|d\delta_{t,\pi\pi}| > 1.5\,\text{ns}$. The differences $d\delta_{t,\pi\text{e}}$ and $d\delta_{t,\text{e}\pi}$ are calculated for events surviving the previous cut. The scatter plot of the two variables is shown in Fig. 2 for Monte Carlo events. The cuts applied on these time differences for the selection of $K_S \to \pi e\nu$ events are illustrated in the figure: $|d\delta_{t,\pi\text{e}}| < 1\,\text{ns}$, $d\delta_{t,\text{e}\pi} > 3\,\text{ns}$; or $|d\delta_{t,\text{e}\pi}| < 1\,\text{ns}$, $d\delta_{t,\pi\text{e}} > 3\,\text{ns}$.

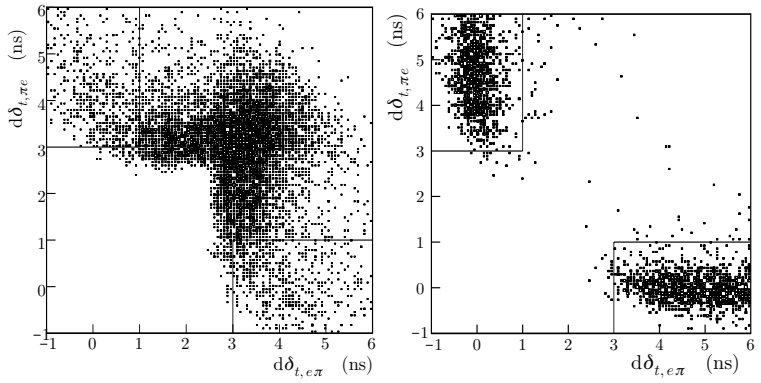

Fig. 2. Scatter plot of the time differences $d\delta_{t,\pi\text{e}}$ vs $d\delta_{t,\text{e}\pi}$ for $e\pi$ and πe mass assignments for $K_S \to \pi^+\pi^-$ (left) and $K_S \to \pi e\nu$ (right) Monte Carlo events.

Finally, for events passing all of the above criteria, we compute the missing energy and momentum E_{miss}, p_{miss}. For $\pi^\pm e^\mp\bar{\nu}(\nu)$ decays, these variables are the neutrino energy and momentum, and satisfy $E_{\text{miss}} = cp_{\text{miss}}$. The distribution of $E_{\text{miss}} - cp_{\text{miss}}$ is shown in Fig. 3 before (left) and after (right) the time-of-flight cuts are imposed. A clear peak at $E_{\text{miss}} - cp_{\text{miss}} = 0$ is evident in the distribution in the right panel and corresponds to a clean signal for $K_S \to \pi e\nu$. Events with $E_{\text{miss}} - cp_{\text{miss}} > 10\,\text{MeV}$ are mostly due to $K_S \to \pi^+\pi^-$ decays in which a pion decays to a muon before reaching the tracking volume. The solid line in the right graph is a fit of the data to the sum of the signal and background spectra simulated using the Monte Carlo (MC). The free fit parameters are the signal and background normalizations. We find:

$$N(\pi^\pm e^\mp\bar{\nu}(\nu)) = 624 \pm 30$$

The quoted error includes the contributions from fluctuations in the signal statistics (± 25), from the background subtraction (± 10), and from the finite statistics of the MC spectra (± 13).

For both $K_S \to \pi^+\pi^-$ (normalization) and $K_S \to \pi e\nu$ (signal) events, contributions to the tagging and selection inefficiencies due to purely geometrical effects have been estimated using MC simulation, while data have been used to estimate the corrections for tracking and trigger inefficiencies. For $K_S \to \pi e\nu$ events, the corrections for vertex reconstruction and time-of-flight π-e identification inefficiencies have also been evaluated using data.

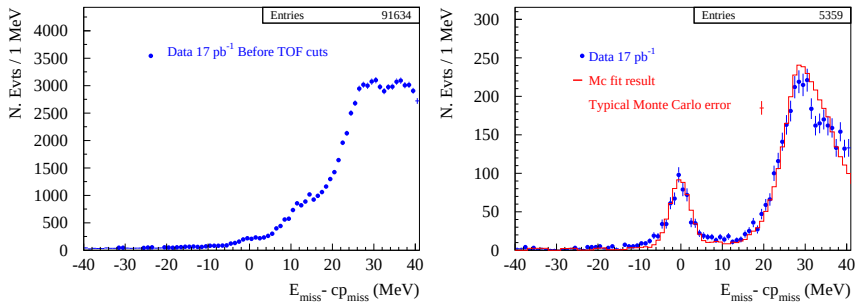

Fig. 3. $E_{\rm miss} - cp_{\rm miss}$ spectrum for $K_S \to \pi e\nu$ candidates before (left) and after (right) TOF cuts.

For $K_S \to \pi^+\pi^-$ events, the MC is used to compute the efficiency after application of the fiducial cuts, since these are fundamentally geometrical. The single-track reconstruction efficiency is obtained in bins of $(p_\perp, \theta)$ from subsamples of $K_S \to \pi^+\pi^-$ events. The ratio of data and MC reconstruction efficiencies is found to be constant throughout the acceptance, and the overall MC efficiency is scaled accordingly. The K_S-K_L final state allows the trigger efficiency to be evaluated directly from data. Because of its high energy, the K_L-crash always fires at least one calorimeter sector. Approximately 40% of the time it fires *two* sectors, giving rise to a valid trigger by itself. Events recognized to have triggered in this way are used to measure the probability that at least one K_S secondary satisfies the trigger together with the K_L-crash cluster, which defines the trigger efficiency in the remaining 60% of events. The $K_S \to \pi^+\pi^-$ selection efficiencies are listed in table 1; for more details see ref. [15].

Table 1
Efficiencies for $\pi^+\pi^-$ and $\pi e\nu$ decays.

$K_S \to \pi^+\pi^-$	Efficiency
Fiducial cuts	0.5755 ± 0.0015
T_0 and trigger	0.976 ± 0.003
$K_S \to \pi e\nu$	Efficiency
Fiducial cuts	0.297 ± 0.005
T_0 and trigger	0.922 ± 0.004
Track-cluster association	0.925 ± 0.006
Time of flight	0.820 ± 0.007
Tag efficiency ratio ($R_{\rm tag}$)	1.024 ± 0.007

For $K_S \to \pi e\nu$ events, the MC is used to evaluate the contributions to the selection inefficiency from the vertex reconstruction, the fiducial cuts, and the $M_{\pi\pi}$ cut. The vertex reconstruction efficiency is also estimated from data,

using events in which the K_L decays into $\pi^{\pm}e^{\mp}\bar{\nu}(\nu)$ near the IP and the K_S decays into $2\pi^0$'s (π^0's do not affect tracking in the drift chamber). The ratio of data and MC efficiencies is used as a scale correction to the MC efficiency. The tracking efficiencies for MC and data have been measured using $K_S \to \pi^+\pi^-$ events, as stated above. The need to extrapolate over a larger interval in the track momenta for $K_S \to \pi e\nu$ events (especially for the electrons) introduces a larger error on the tracking efficiency correction in this case.

The track-to-cluster association efficiency $\varepsilon_{\rm tca}$ includes both the probability that the particle reaching the calorimeter (π^+, π^-, $e^{\mp}$, or $\mu^{\mp}$) deposits enough energy to be detected, and the probability that the track and cluster are correctly associated during reconstruction. The trigger efficiency $\varepsilon_{\rm trg}$ is given by the probability that one of the K_S clusters together with the K_L-crash cluster triggers the event. The overall corrections for $\varepsilon_{\rm tca}$, $\varepsilon_{\rm trg}$, and the time-of-flight identification efficiency are obtained using a high-purity ($> 99.7\%$) sample of $K_L \to \pi e\nu$, $K_S \to \pi^+\pi^-$ events in which the K_L decays near the IP and the K_S decay generates the trigger. Such $K_L\ell 3$-*gold* events can be selected using track kinematics only, with essentially no recourse to calorimeter information. Independent estimates for $\varepsilon_{\rm tca}$ and $\varepsilon_{\rm trg}$ parameterized in the variables of each track can be obtained from samples of $\phi \to \pi^+\pi^-\pi^0$, $K_S \to \pi^+\pi^-$, and $K_L\ell 3$-gold events. For all of these event types, reconstruction is possible whether or not one of the tracks leaves a cluster in the calorimeter. The efficiencies are then parameterized separately for each particle type, and used to weight the MC-generated semileptonic events to obtain an average correction. The results obtained with the two methods agree within errors. The overall efficiency $\epsilon_{\rm tot}^{\pi e\nu}$ for the detection of signal events is 0.208 ± 0.004. The various contributions are separately listed in table 1; for more details see ref. [16].

In principle, the K_L-crash identification efficiency cancels out in the ratio of the number of selected $K_S \to \pi e\nu$ and $K_S \to \pi^+\pi^-$ events. In practice, since the event T_0 is obtained from the K_S and the K_L is recognized by its time of flight, there is a small dependence of the K_L-crash identification efficiency on the K_S decay mode. A correction for this effect is obtained by studying the accuracy of the T_0 determination in each case. For the case of $K_S \to \pi e\nu$, this study is performed using $K_L\ell 3$-gold events in which the topology of the $K_L \to \pi e\nu$ decay is manipulated to reflect the K_S decay length distribution, and in which the true T_0 is unambiguous (both the π^+ and π^- from the K_S give the same T_0). For the case of $K_S \to \pi^+\pi^-$, this study is performed using $K_L \to \pi^+\pi^-\pi^0$, $K_S \to \pi^+\pi^-$ events, in which the K_L decay gives an unambiguous estimate of the event T_0. Such events can be recognized without knowledge of the event T_0 *a priori*. The ratio $R_{\rm tag}$ of the tagging efficiencies for $K_S \to \pi e\nu$ and $K_S \to \pi^+\pi^-$ is found to differ from unity by $\sim 2\%$ (see table 1).

The value for BR($K_S \to \pi e\nu$) is obtained by normalizing the number of signal

events to the number of $K_S \to \pi^+\pi^-$ events in the same data set, correcting for the total selection efficiencies and the ratio $R_{\rm tag}$ of tagging efficiencies, and using the present experimental value for BR($K_S \to \pi^+\pi^-$) [5]:

$$\mathrm{BR}(K_S \to \pi e\nu) = \frac{N^{\pi e\nu}}{N^{\pi\pi}} \times \frac{\varepsilon^{\pi\pi}_{\rm tot}}{\varepsilon^{\pi e\nu}_{\rm tot}} \times \frac{1}{R_{\rm tag}} \times \mathrm{BR}(K_S \to \pi^+\pi^-).$$

We obtain

$$\mathrm{BR}(K_S \to \pi^\pm e^\mp \bar{\nu}(\nu)) = (6.91 \pm 0.34_{\rm stat} \pm 0.15_{\rm syst}) \times 10^{-4},$$

in agreement with the expectation from the Standard Model. The contributions to the error in our measurement are given in table 2.

Table 2
Fractional errors on BR($K_S \to \pi e\nu$).

Source	Error, %
Statistics, signal and background	4.9
$K_S \to \pi e\nu$ selection	
Tracking and vertex efficiency	1.4
MC preselection efficiency	0.5
Track-cluster, T_0 and trigger	0.7
Time-of-flight cuts	0.9
$K_S \to \pi^+\pi^-$ selection	
Acceptance	0.2
Tracking	0.2
T0 and Trigger	0.3
Tag efficiency ratio ($R_{\rm tag}$)	0.7
BR($K_S \to \pi^+\pi^-$)	0.4
Total error	5.3

This analysis demonstrates that KLOE can isolate a very pure sample of $K_S \to \pi e\nu$ decays. The overall selection efficiency for $K_S \to \pi e\nu$ decays among K_S-tagged events is 0.208 ± 0.004, due in large part to the tight fiducial cuts imposed on the decays of interest.

We thank the DAΦNE team for their efforts in maintaining low background running conditions and their collaboration during all data-taking. We also thank F. Fortugno for his efforts in ensuring good operations of the KLOE computing facilities. This work was supported in part by EURODAPHNE,

contract FMRX-CT98-0169; by the German Federal Ministry of Education and Research (BMBF) contract 06-KA-957; by Graduiertenkolleg 'H.E. Phys. and Part. Astrophys.' of Deutsche Forschungsgemeinschaft, Contract No. GK 742; by INTAS, contracts 96-624, 99-37; and by TARI, contract HPRI-CT-1999-00088.

References

[1] C. O. Dib, B. Guberina, Phys. Lett. B255 (1991) 113.

[2] M. Luke, Phys. Lett. B256 (1991) 265.

[3] L. Maiani, CP and CPT violation in neutral kaon decays, in: L. Maiani, G. Pancheri, N. Paver (Eds.), The Second DAΦNE Physics Handbook, Vol. 1, 1995, p. 3.

[4] P. Franzini, in: D. Cline, W. Scientific (Eds.), Proc. Symp. *Flavour Changing Neutral Currents: Present and Future Studies*, Santa Monica, 1997, p. 345.

[5] D. E. Groom, et al., Eur. Phys. J. C15 (2000) 1.

[6] R. Akhmetshin, et al., Phys. Lett. B456 (1999) 90.

[7] KLOE collaboration, M. Adinolfi, *et al.*, KLOE: A general purpose detector for DAFNE, LNF-92/019 (IR).

[8] KLOE collaboration, M. Adinolfi, *et al.*, The KLOE detector, technical proposal, LNF-93/002 (IR).

[9] S. Guiducci, Status of DAΦNE, in: P. Lucas, S. Webber (Eds.), Proc. of the 2001 Particle Accelerator Conference - Chicago, IL U.S.A., 2001, p. 353.

[10] I. Dunietz, J. Hauser, J. Rosner, Phys. Rev. D35 (1987) 2166.

[11] N. Brown, F. E. Close, Scalar mesons and kaons in ϕ radiative decay & their implications for studies of CP violation at DAΦNE, in: L. Maiani, G. Pancheri, N. Paver (Eds.), The DAΦNE Physics Handbook, Vol. 2, 1992, p. 447.

[12] KLOE collaboration, M. Adinolfi, *et al.*, Nucl. Inst. Meth. A, in press.

[13] KLOE collaboration, M. Adinolfi, *et al.*, Nucl. Inst. Meth. A482 (2002) 363.

[14] KLOE collaboration, M. Adinolfi, *et al.*, The KLOE trigger system, LNF Report LNF-02.

[15] M. Palutan, T. Spadaro, P. Valente, Measurement of $\Gamma(K_S \to \pi^+\pi^-)/\Gamma(K_S \to \pi^0\pi^0)$ with KLOE 2000 data, KLOE note 174 (2002).
URL `http://www.lnf.infn.it/kloe/pub/knote/kn174.ps.gz`

[16] C. Gatti, T. Spadaro, Measurement of BR($K \to \pi^\pm e^\mp \bar{\nu}(\nu)$), KLOE note 176 (2002).
URL `http://www.lnf.infn.it/kloe/pub/knote/kn176.ps.gz`